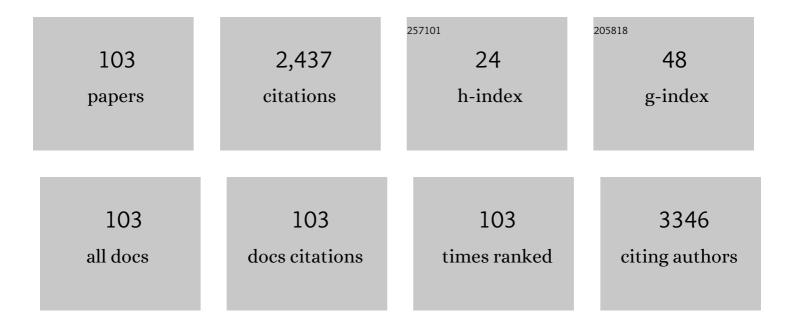
List of Publications by Year in descending order

Source: https://exaly.com/author-pdf/7117706/publications.pdf Version: 2024-02-01



#	Article	IF	CITATIONS
1	A band-gap-graded CZTSSe solar cell with 12.3% efficiency. Journal of Materials Chemistry A, 2016, 4, 10151-10158.	5.2	260
2	Hysteresis-less mesoscopic CH3NH3PbI3 perovskite hybrid solar cells by introduction of Li-treated TiO2 electrode. Nano Energy, 2015, 15, 530-539.	8.2	246
3	Effect of solid-H ₂ S gas reactions on CZTSSe thin film growth and photovoltaic properties of a 12.62% efficiency device. Journal of Materials Chemistry A, 2019, 7, 25279-25289.	5.2	229
4	Highly reproducible planar Sb ₂ S ₃ -sensitized solar cells based on atomic layer deposition. Nanoscale, 2014, 6, 14549-14554.	2.8	182
5	Effect of Polyethylene Glycol on Gene Delivery of Polyethylenimine Biological and Pharmaceutical Bulletin, 2003, 26, 492-500.	0.6	164
6	Effects of Na and MoS ₂ on Cu ₂ ZnSnS ₄ thinâ€film solar cell. Progress in Photovoltaics: Research and Applications, 2015, 23, 862-873.	4.4	108
7	Flexible Cu2ZnSn(S,Se)4 solar cells with over 10% efficiency and methods of enlarging the cell area. Nature Communications, 2019, 10, 2959.	5.8	100
8	Ultrathin ZrO2 on LiNi0.5Mn0.3Co0.2O2 electrode surface via atomic layer deposition for high-voltage operation in lithium-ion batteries. Applied Surface Science, 2019, 484, 701-709.	3.1	65
9	8.01% CuInGaSe2 solar cells fabricated by air-stable low-cost inks. Physical Chemistry Chemical Physics, 2012, 14, 11154.	1.3	64
10	Void and secondary phase formation mechanisms of CZTSSe using Sn/Cu/Zn/Mo stacked elemental precursors. Nano Energy, 2019, 59, 399-411.	8.2	61
11	Preparation and charateristics of Nafion membrane coated with a PVdF copolymer/recast Nafion blend for direct methanol fuel cell. Journal of Power Sources, 2006, 159, 524-528.	4.0	55
12	A discussion on the origin and solutions of hysteresis in perovskite hybrid solar cells. Journal Physics D: Applied Physics, 2016, 49, 473001.	1.3	45
13	Solution-processed Cu ₂ ZnSnS ₄ absorbers prepared by appropriate inclusion and removal of thiourea for thin film solar cells. RSC Advances, 2014, 4, 9118-9125.	1.7	44
14	Perspective: Understanding of ripening growth model for minimum residual PbI2 and its limitation in the planar perovskite solar cells. APL Materials, 2016, 4, .	2.2	43
15	Sodium Effects on the Diffusion, Phase, and Defect Characteristics of Kesterite Solar Cells and Flexible Cu ₂ ZnSn(S,Se) ₄ with Greater than 11% Efficiency. Advanced Functional Materials, 2021, 31, 2102238.	7.8	36
16	Controlled synthesis of (<i>hk</i> 1) preferentially oriented Sb ₂ Se ₃ rod arrays by co-evaporation for photovoltaic applications. Journal of Materials Chemistry A, 2019, 7, 25900-25907.	5.2	34
17	Quasi-solid state electrolyte for semi-transparent bifacial dye-sensitized solar cell with over 10% power conversion efficiency. Journal of Power Sources, 2017, 361, 87-95.	4.0	31
18	A coated Nafion membrane with a PVdF copolymer/Nafion blend for direct methanol fuel cells (DMFCs). Solid State Ionics, 2005, 176, 3027-3030.	1.3	30

#	Article	IF	CITATIONS
19	Proton conducting semi-IPN based on Nafion and crosslinked poly(AMPS) for direct methanol fuel cell. Electrochimica Acta, 2004, 50, 588-593.	2.6	29
20	Dimerization behavior of cinnamate group attached to flexible polymer backbone and its effect on the molecular orientation. Chemical Physics Letters, 2004, 394, 238-243.	1.2	28
21	Two different reaction mechanisms of cinnamate side groups attached to the various polymer backbones. Polymer, 2006, 47, 2314-2321.	1.8	27
22	Nanostructured p-type CZTS thin films prepared by a facile solution process for 3D p–n junction solar cells. Nanoscale, 2015, 7, 11182-11189.	2.8	27
23	Flexible high-efficiency CZTSSe solar cells on stainless steel substrates. Journal of Materials Chemistry A, 2019, 7, 24891-24899.	5.2	27
24	Approach to Transparent Photovoltaics Based on Wide Band Gap Sb ₂ S ₃ Absorber Layers and Optics-Based Device Optimization. ACS Applied Energy Materials, 2020, 3, 12644-12651.	2.5	25
25	Effect of hafnium addition on the electrical properties of indium zinc oxide thin film transistors. Thin Solid Films, 2011, 519, 6815-6819.	0.8	24
26	Systematic control of nanostructured interfaces of planar Sb 2 S 3 solar cells by simple spin-coating process and its effect on photovoltaic properties. Journal of Industrial and Engineering Chemistry, 2017, 56, 196-202.	2.9	24
27	Synthesis, photo-reaction and photo-induced liquid crystal alignment of soluble polyimide with pendant cinnamate group. Liquid Crystals, 2000, 27, 1343-1356.	0.9	22
28	High performance and the low voltage operating InGaZnO thin film transistor. Current Applied Physics, 2010, 10, e157-e160.	1.1	22
29	Photo-induced liquid crystal alignment of poly(vinyl cinnamate) and fluorinated polyimide blends. Materials Science and Engineering C, 2004, 24, 181-184.	3.8	21
30	Spin-Coating Process of an Inorganic Sb ₂ S ₃ Thin Film for Photovoltaic Applications. Journal of Nanoscience and Nanotechnology, 2016, 16, 10763-10766.	0.9	21
31	Mechanism of Photo-Induced Liquid Crystal Alignment on a Poly(vinyl cinnamate) Thin Layer. Polymer Journal, 2001, 33, 9-12.	1.3	16
32	Photo-induced liquid crystal alignment on polyimide containing fluorinated groups. Liquid Crystals, 2002, 29, 243-250.	0.9	16
33	Controlled growth of organic–inorganic hybrid CH ₃ NH ₃ PbI ₃ perovskite thin films from phase-controlled crystalline powders. RSC Advances, 2016, 6, 104359-104365.	1.7	16
34	Novel Photo-Alignment Polymer Layer Capable of Charge Transport. Macromolecular Chemistry and Physics, 2004, 205, 2245-2251.	1.1	15
35	Low Voltage, High Performance Thin Film Transistor with HfInZnO Channel and HfO[sub 2] Gate Dielectric. Electrochemical and Solid-State Letters, 2010, 13, H274.	2.2	15
36	Carbon black effect on the acoustic properties of nitrile butadiene rubber. Journal of Applied Polymer Science, 2004, 94, 678-683.	1.3	14

#	Article	lF	CITATIONS
37	Effects of Ti addition on sol-gel derived InO and InZnO thin film transistors. Current Applied Physics, 2012, 12, e24-e28.	1.1	13
38	The optical and structural properties of CuIn1â^'x Ga x Se2 thin films fabricated with various Ga contents by using the co-evaporation technique. Journal of the Korean Physical Society, 2012, 60, 1708-1712.	0.3	13
39	Relationship between pretilt angle and surface energy of the blended films based on poly(vinyl) Tj ETQq1 1 0.7	′84314.rgB ⁻ 2.1	Г /Overlock I(12
40	Effects of annealing on structural and electrical properties of sub-micron thick CIGS films. Current Applied Physics, 2013, 13, S135-S139.	1.1	12
41	Molecular Orientation of Liquid Crystal on Polymer Blends of Coumarin and Naphthalenic Polyimide. Polymer Bulletin, 2008, 61, 383-390.	1.7	11
42	Enhanced Power Conversion Efficiency of Dye-Sensitized Solar Cells by Band Edge Shift of TiO2 Photoanode. Molecules, 2020, 25, 1502.	1.7	11
43	Atomic Layer Deposition of Ultrathin ZnO Films for Hybrid Window Layers for Cu(Inx,Ga1â^'x)Se2 Solar Cells. Nanomaterials, 2021, 11, 2779.	1.9	10
44	Ultraviolet embossed alignment layers having patterned spacers for flexible liquid crystal display. Displays, 2008, 29, 478-481.	2.0	9
45	Photo-induced liquid crystal alignment on polyimide containing fluorine group. Synthetic Metals, 2001, 117, 277-279.	2.1	8
46	Pixel-isolation liquid crystals formed by polarization-selective UV-curing of a prepolymer containing cinnamate oligomer. Optics Express, 2010, 18, 11737.	1.7	8
47	Structure control of lattice-patterned liquid crystals–polymer composites prepared by polarization-selective UV-curing through the addition of a fluorinated acrylate monomer. Microelectronic Engineering, 2013, 103, 42-48.	1.1	8
48	Mesoporous TiO ₂ hierarchical structures: preparation and efficacy in solar cells. RSC Advances, 2017, 7, 49057-49065.	1.7	8
49	Facile growth of a Sb ₂ Se ₃ nanorod array induced by a MoSe ₂ interlayer and its application in 3D p–n junction solar cells. Materials Advances, 2022, 3, 978-985.	2.6	7
50	Effect of the shape of imprinted alignment layer on the molecular orientation of liquid crystal. Materials Science and Engineering C, 2007, 27, 798-801.	3.8	6
51	The effect of bi-component acrylate prepolymers on the phase separation and electro-optical properties of pixel-isolated liquid crystals. Displays, 2011, 32, 334-337.	2.0	6
52	Effect of hot-pressing on an electrospun TiO2electrode for dye-sensitized solar cells. Applied Physics Express, 2014, 7, 072301.	1.1	6
53	Effect of composition and synthetic route on the microstructure of biodegradable diblock copolymer, poly(ε-caprolactone-co-L-lactide)-b-poly(ethylene glycol). Macromolecular Research, 2008, 16, 231-237.	1.0	5
54	Effect of molecular weight of biscinnamated poly(ethylene glycol) oligomers on the photocycloaddition reaction. Macromolecular Research, 2010, 18, 614-617.	1.0	5

#	Article	IF	CITATIONS
55	Electroreflectance study of CuIn1â^'xGaxSe2 thin film solar cells. Current Applied Physics, 2014, 14, 318-321.	1.1	5
56	Effect of photoreactivity of polyimide on the molecular orientation of liquid crystals on photoreactive polymer/polyimide blends. Liquid Crystals, 2004, 31, 1601-1611.	0.9	4
57	Photo-induced liquid crystal alignment on imide oligomer containing cinnamate group. Materials Science and Engineering C, 2004, 24, 195-199.	3.8	4
58	Effects of Sodium Dodecyl Sulfate as a Co-Adsorbate on the Performance of Dye-Sensitized Solar Cells. Journal of Nanoscience and Nanotechnology, 2015, 15, 7727-7732.	0.9	4
59	Crystallization Behavior of Solution-Processed CIGSe Thin Film Semiconductor by Stepwise Annealing Process. Journal of Nanoscience and Nanotechnology, 2015, 15, 2490-2494.	0.9	4
60	Characterization of in-situ annealed sub-micron thick Cu(In,Ga)Se2 thin films. Thin Solid Films, 2015, 590, 330-334.	0.8	4
61	Preferential (100)-oriented CH ₃ NH ₃ Pbl ₃ perovskite film formation by flash drying and elucidation of formation mechanism. RSC Advances, 2016, 6, 94502-94509.	1.7	4
62	CZTSSe Formation Mechanism Using a Cu/Zn/SnS Stacked Precursor: Origin of Triple CZTSSe Layer Formation. ACS Applied Materials & Interfaces, 2020, 12, 46037-46044.	4.0	4
63	Effect of Metal-Precursor Stacking Order on Volume-Defect Formation in CZTSSe Thin Film: Formation Mechanism of Blisters and Nanopores. ACS Applied Materials & Interfaces, 2022, 14, 30649-30657.	4.0	4
64	The Electro-Optical Behavior of Liquid Crystal Molecules on the Surface of SiO2 Inorganic Thin Films. Journal of Nanoscience and Nanotechnology, 2009, 9, 6938-42.	0.9	3
65	Effects of Addition of Ta and Y lons to InZnO Thin Film Transistors by Sol–Gel Process. Journal of Nanoscience and Nanotechnology, 2013, 13, 4211-4215.	0.9	3
66	Light Harvest Properties of Dye-Sensitized Solar Cells with Different Spatial Configurations of Reflecting Layer. Journal of Nanoscience and Nanotechnology, 2013, 13, 7123-7126.	0.9	3
67	Effects of Ta Addition Through Co-Sputtering on the Electrical Characteristics of Indium Tin Oxide Thin Film Transistors. Journal of Nanoscience and Nanotechnology, 2015, 15, 386-390.	0.9	3
68	Determination of Carrier Lifetimes in Organic-Inorganic Hybrid Solar Cells Based on Sb2S3 by Using the Time-Resolved Photocurrent. Journal of the Korean Physical Society, 2018, 72, 709-715.	0.3	3
69	Design of Grating Al2O3 Passivation Structure Optimized for High-Efficiency Cu(In,Ga)Se2 Solar Cells. Sensors, 2021, 21, 4849.	2.1	3
70	Effect of Soft-annealing on the Properties of CICSe Thin Films Prepared from Solution Precursors. Bulletin of the Korean Chemical Society, 2013, 34, 1473-1476.	1.0	3
71	Effect of Plasticization of Poly(Vinyl Cinnamate) on Liquid Crystal Orientation Stability. Japanese Journal of Applied Physics, 2005, 44, L412-L415.	0.8	2
72	Simultaneous fabrication of an alignment layer and a wall structure for a liquid crystal display by solvent-assisted micromolding. Macromolecular Research, 2012, 20, 453-458.	1.0	2

#	Article	IF	CITATIONS
73	Contact-free method to prepare photoalignment layers with spacers for flexible liquid crystal displays. Microelectronic Engineering, 2012, 96, 67-70.	1.1	2
74	Particulate counter electrode system for enhanced light harvesting in dye-sensitized solar cells. Optical Materials Express, 2013, 3, 739.	1.6	2
75	Phase separation structure and interfacial properties of latticeâ€patterned liquid crystal–polymer composites prepared from multicomponent prepolymers. Polymer International, 2014, 63, 214-220.	1.6	2
76	Double-layered TiO_2 photoelectrode with particulate structure prepared by one-step soaking method. Optical Materials Express, 2014, 4, 2401.	1.6	2
77	Enhanced Performance of Polymer Solar Cells with a Fluorocyanophenyl Compound as an Additive. Journal of Nanoscience and Nanotechnology, 2014, 14, 9219-9223.	0.9	2
78	Effect of Hydrogen Post-Annealing on Transparent Conductive ITO/Ga2O3 Bi-Layer Films for Deep Ultraviolet Light-Emitting Diodes. Journal of Nanoscience and Nanotechnology, 2015, 15, 7777-7780.	0.9	2
79	Improved Photovoltaic Properties of Dye-Sensitized Solar Cells with KNO ₃ -Modified Photoelectrodes. Journal of Nanoscience and Nanotechnology, 2015, 15, 8859-8863.	0.9	2
80	Controlled fabrication of mesoporous TiO ₂ hierarchical structures as scattering layers to enhance the power conversion efficiency of dye-sensitized solar cells. Physical Chemistry Chemical Physics, 2016, 18, 30254-30260.	1.3	2
81	Effects of TiO2:MgO-Mixed Overlayer on the Performance of Dye-Sensitized Solar Cells. Journal of Nanoscience and Nanotechnology, 2016, 16, 8575-8579.	0.9	2
82	Spin-Coated Uniform Sb ₂ S ₃ Thin Films for Photovoltaic Applications by Solvent Engineering. Nanoscience and Nanotechnology Letters, 2017, 9, 1327-1331.	0.4	2
83	Static charge reducible liquid crystal alignment layer based on PAAc doped PMDA-ODA/polyaniline blend. Synthetic Metals, 2001, 117, 271-272.	2.1	1
84	Lattice-patterned LC-polymer composites containing various nanoparticles as additives. Nanoscale Research Letters, 2012, 7, 46.	3.1	1
85	Heat Resistant Polymer Matrix Containing Acrylo-Polyhedral Silsesquioxane for Erbium-Doped Waveguide Amplifier Applications. Molecular Crystals and Liquid Crystals, 2013, 586, 33-42.	0.4	1
86	Effect of Ta Addition of Co-sputtered Amorphous Tantalum Indium Zinc Oxide Thin Film Transistors with Bias Stability. Journal of Nanoscience and Nanotechnology, 2014, 14, 8163-8166.	0.9	1
87	Effect of Sulfurization Temperature on Solution-Processed Cu ₂ ZnSnS ₄ Thin Films. Journal of Nanoscience and Nanotechnology, 2015, 15, 2486-2489.	0.9	1
88	Effect of TiCl ₄ Post-Treatment on the Embedded-Type TiO ₂ Nanotubes Dye-Sensitized Solar Cells. Journal of Nanoscience and Nanotechnology, 2015, 15, 7845-7847.	0.9	1
89	Performance Enhancement of Dye-Sensitized Solar Cells with KMnO ₄ -Modified Photoelectrodes. Journal of Nanoscience and Nanotechnology, 2016, 16, 10420-10425.	0.9	1
90	Low-Cost Nanoporous Cu ₂ ZnSnS ₄ Thin-Film Counter Electrode for Dye-Sensitized Solar Cells. Journal of Nanoscience and Nanotechnology, 2016, 16, 10490-10494.	0.9	1

#	Article	IF	CITATIONS
91	Enhanced Performance of Dye-Sensitized Solar Cells Based on Electrospun TiO2 Electrode. Journal of Nanoscience and Nanotechnology, 2017, 17, 8117-8121.	0.9	1
92	Retardation of Charge Recombination Between Hole Conductors and TiCl ₄ :BaCl ₂ -Modified Photoelectrodes in TiO ₂ -Based Solar Cells. Journal of Nanoscience and Nanotechnology, 2017, 17, 8144-8148.	0.9	1
93	Inverted Polymer Solar Cells with a Poly(diallyldimethylammonium chloride) as an Electron Collecting Layer. Science of Advanced Materials, 2014, 6, 2334-2337.	0.1	1
94	Thermal Reaction of Cinnamate Oligomers and Their Effect on the Orientational Stability of Liquid Crystals. Japanese Journal of Applied Physics, 2006, 45, 6442-6444.	0.8	0
95	Effect of sputtering condition on the surface properties of silicon oxide thin films prepared for liquid crystal alignment layers. Displays, 2010, 31, 93-98.	2.0	ο
96	Pixel-Isolation Walls of Liquid Crystal Display Based on Prepolymer Containing Vinyl Cinnamate. Journal of Nanoscience and Nanotechnology, 2012, 12, 3360-3363.	0.9	0
97	Investigation of Crystallization Behavior of CIG-Se Bi-Layer Thin Films. Journal of Nanoscience and Nanotechnology, 2012, 12, 3488-3491.	0.9	Ο
98	Preparation and Physical Properties of Erbium-Doped Polymer Patterns by Micromolding in Capillaries for Optical Waveguide Amplifiers. Molecular Crystals and Liquid Crystals, 2012, 564, 222-232.	0.4	0
99	Incorporation of Potassium Water Class on Photoelectrodes and Its Effects on the Performance of Dye-Sensitized Solar Cells. Journal of Nanoscience and Nanotechnology, 2015, 15, 8854-8858.	0.9	ο
100	Correlation Between Chemical Composition and Efficiency of Cu2ZnSnS4 Solar Cells Prepared by a Solution Process. Journal of Nanoscience and Nanotechnology, 2016, 16, 8648-8653.	0.9	0
101	Effect of Morphology of Solution-Processed Precursor Films on Cu ₂ ZnSnS ₄ Thin Film Solar Cells. Journal of Nanoscience and Nanotechnology, 2016, 16, 10758-10762.	0.9	Ο
102	Fabrication of Dye-Sensitized Solar Cells Based on Embedded Photoelectrodes of TiO ₂ Nanotube-Nanoparticles Composite. Journal of Nanoscience and Nanotechnology, 2016, 16, 10716-10719.	0.9	0
103	Effects of Thickness of Electrosprayed Spherical TiO ₂ Photoelectrodes on the Performance of Dye-Sensitized Solar Cells. Science of Advanced Materials, 2016, 8, 640-644.	0.1	Ο